

Tide and Tidal Current in the Yellow/East China Seas *

Tetsuo YANAGI** and Kouichi INOUE**

Abstract: The four major components of tides and tidal currents, M_2 , S_2 , K_1 and O_1 in the Yellow/East China Seas are well reproduced except amphidromic points of M_2 and S_2 in Liautung Bay with use of the horizontal two-dimensional numerical model with a cartesian coordinate of β -plane. The curvature of the earth does not affect the tidal phenomena there. The characteristics of tides and tidal currents in the Yellow/East China Seas are discussed.

1. Introduction

The Yellow/East China Seas (including Bohai Sea) are one of the largest shelf sea in the world (Fig. 1). Much land-derived materials flow into this shelf sea from large rivers such as Huanghe, Changjiang and so on. They are advected by residual flow and dispersed mainly by tidal current, which is the most dominant flow there, and some of them deposit to the bottom of this shelf sea and others flow out to the Pacific Ocean through the shelf edge or to the Japan Sea through the Tsushima Strait. It is very important to reveal the characteristics of tidal current in the Yellow/East Chian Seas in order to clarify the material transport there.

AN (1977) carried out a numerical experiment with the cartesian co-ordinate of f -plane including the tide-generating potentials on M_2 tide in the Yellow Sea. CHOI (1980) revealed the characteristics of four major tidal components, M_2 , S_2 , K_1 and O_1 in the Yellow/East Chian Seas with use of the horizontal two-dimensional numerical model under the spherical co-ordinate of β -plane neglecting the tide-generating potentials. Moreover, CHOI (1984) revealed the three-dimensional structure of M_2 tidal current in the Yellow/East Chian Seas with use of linear numerical model except a quadratic bottom friction.

As for field observation of tides there, the work by OGURA (1933) is very famous and it has been used for the verification of numerical

experiments. Recently, NISHIDA (1980) reconstructed the co-tidal and co-range charts of four major tidal components there with new tidal data.

Here we try to reveal the characteristics of tides and tidal currents in the Yellow/East Chian Seas with use of two-dimensional numerical model under the cartesian co-ordinate of β -plane. The aim of this paper is to compare our results with those by CHOI (1980) under the spherical co-ordinate and to investigate the effect of earth's curvature to the tidal phenomena in the Yellow/East Chian Seas.

2. Field data

The amplitude spectra of tides at two representative stations (OGURA, 1941) are shown in Fig. 2. M_2 tide is the most dominant and S_2 , N_2 , K_1 , and O_1 components are dominant. Though S_a component is also dominant, we do not treat it in this paper, because it is mainly governed by meteorological effects, that is, by the seasonal variations in water temperature, air pressure and sea surface wind. Such meteorological effects on the currents there were already investigated by YANAGI and TAKAHASHI (1993). Therefore, we try to reproduce major components of M_2 , S_2 , N_2 , K_1 and O_1 tides and tidal currents in the Yellow/East Chian Seas in this paper.

3. Numerical model

The horizontal two-dimensional momentum and continuity equations for tide and tidal current in the homogeneous fluid under the cartesian co-ordinate are as follows (YANAGI and OKAMOTO, 1985),

* Received May 4, 1994

** Department of Civil and Ocean Engineering, Ehime University, Bunkyo 3 Matsuyama 790, Japan

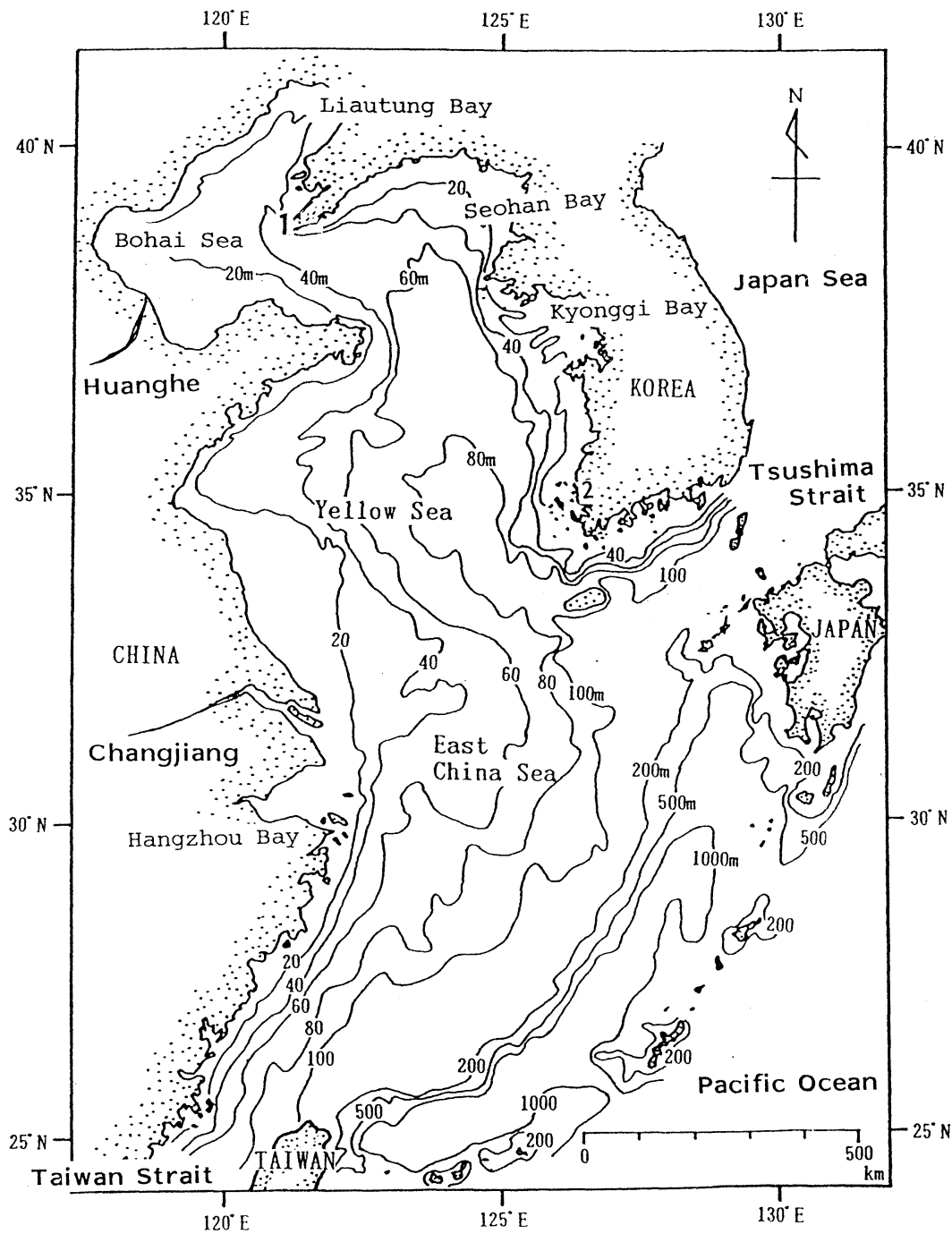


Fig. 1. Yellow/East China Seas. Numbers 1 (Ryozyun), 2 (Gunsan) show the tidal stations.

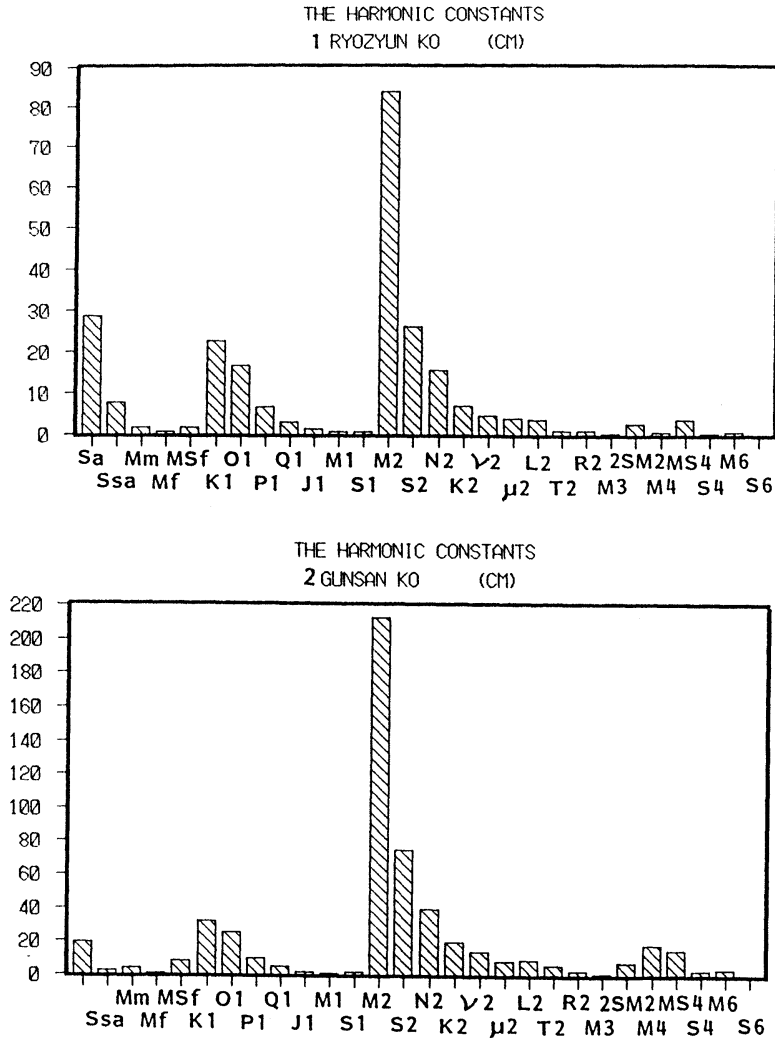


Fig. 2. Tidal amplitude spectra at representative two stations 1 (Ryozyun) and 2 (Gunsan).

$$\frac{\partial u}{\partial t} + (u \cdot \nabla)u + fK \times u = -g \nabla \eta - \frac{\gamma_b^2 |u| u}{H + \eta} + \nu \nabla^2 u \quad (1)$$

$$\frac{\partial \eta}{\partial t} + \nabla \cdot \{(H + \eta)u\} = 0 \quad (2)$$

Here u is the depth-averaged velocity vector, t time, ∇ the horizontal differential operator, f the Coriolis parameter and $f = f_0 + \beta$ ($f_0 = 7.7 \times 10^{-5} \text{ s}^{-1}$ at 33° N and $\beta = 0.23 \times 10^{-5} \text{ s}^{-1} \text{ degree}^{-1}$), y the difference of latitude from 33° N , K the locally vertical unit vector, g ($=980 \text{ cm s}^{-2}$) the

gravitational acceleration, η the sea surface elevation above the mean sea surface, γ_b^2 ($=0.0026$) the bottom frictional coefficient, ν ($=10^7 \text{ cm}^2 \text{ s}^{-1}$) the horizontal eddy viscosity, and H the local water depth.

Equations (1) and (2) are approximated by finite-differences and are solved by the primitive method. The grid size is $25 \text{ km} \times 25 \text{ km}$. The observed tidal amplitude and phase lag are given along three open boundaries, Tsushima Strait, 300 m iso-bath and Taiwan Strait shown in Fig. 3, on the basis of co-tidal and co-range

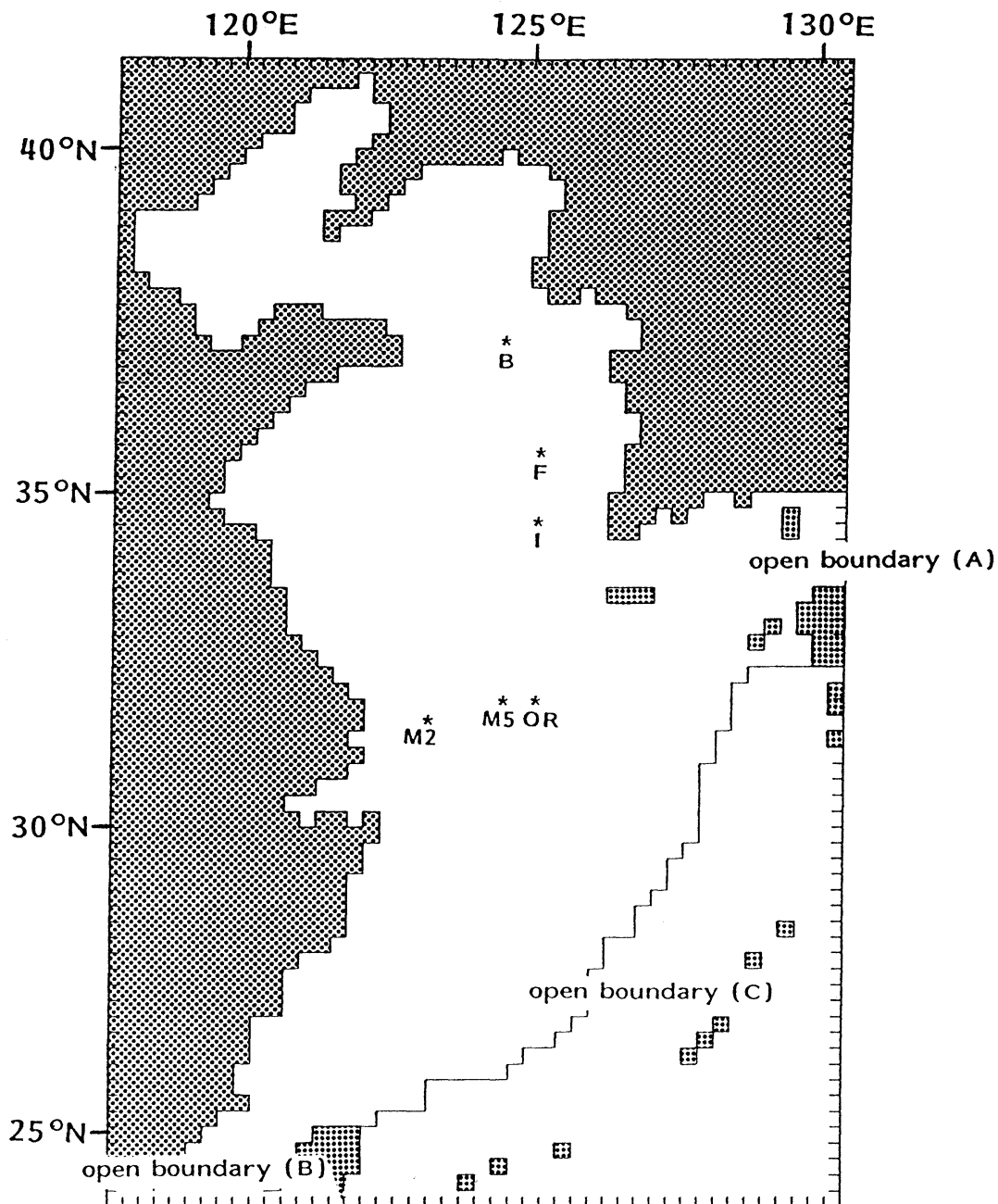


Fig. 3. Numerical model with open boundaries. The symbol shows the observation station of tidal current and its result is shown in Fig. 6.

charts by NISHIDA (1980). The quasi-steady state is obtained four tidal cycles after the beginning of the calculation and the harmonic analysis of sea surface elevation and current

field is carried out at the 5th tidal cycle.

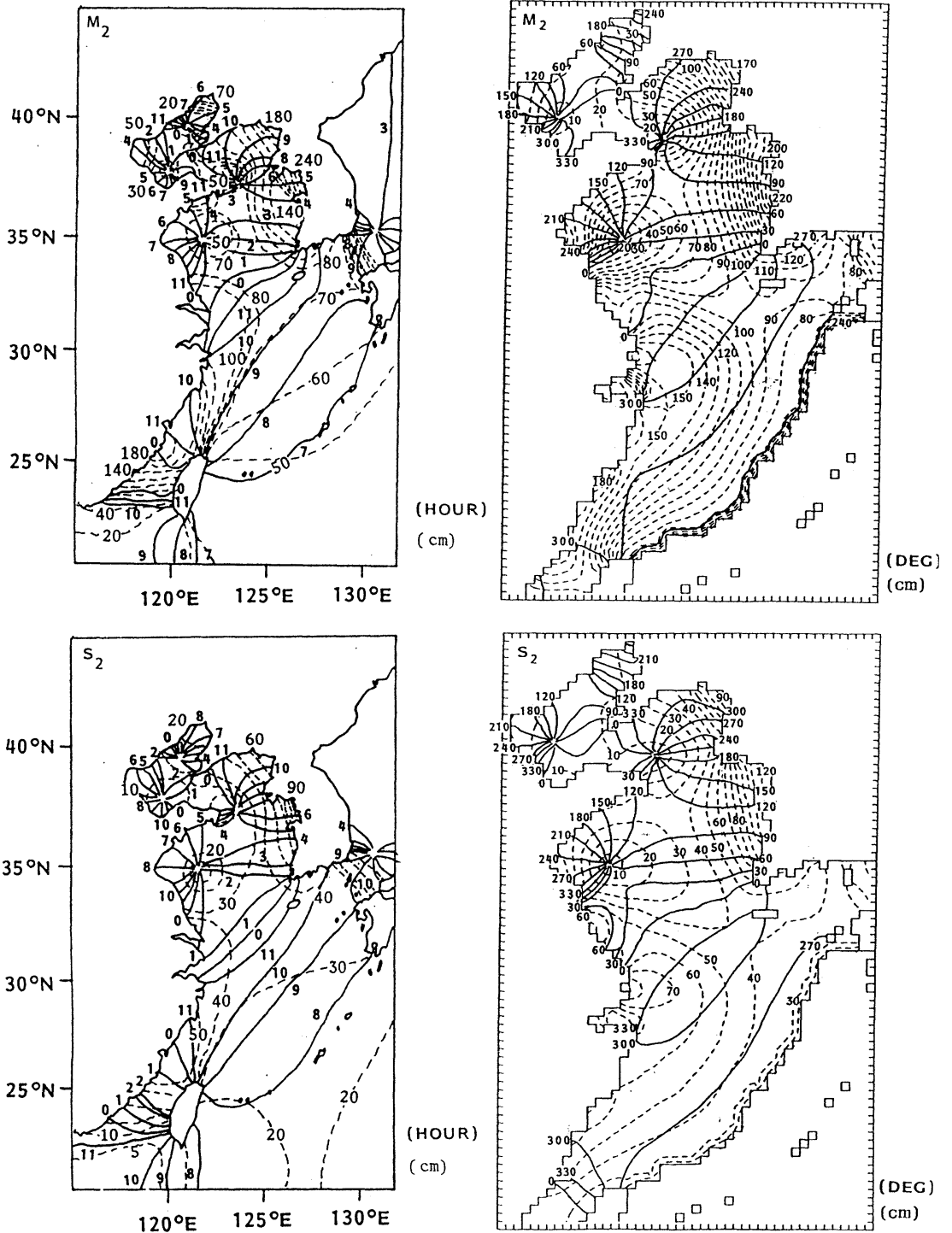


Fig. 4. Observed co-tidal (full line) and co-range (broken line) charts (left) and calculated ones right of M_2 and tides in the Yellow/East China Seas.

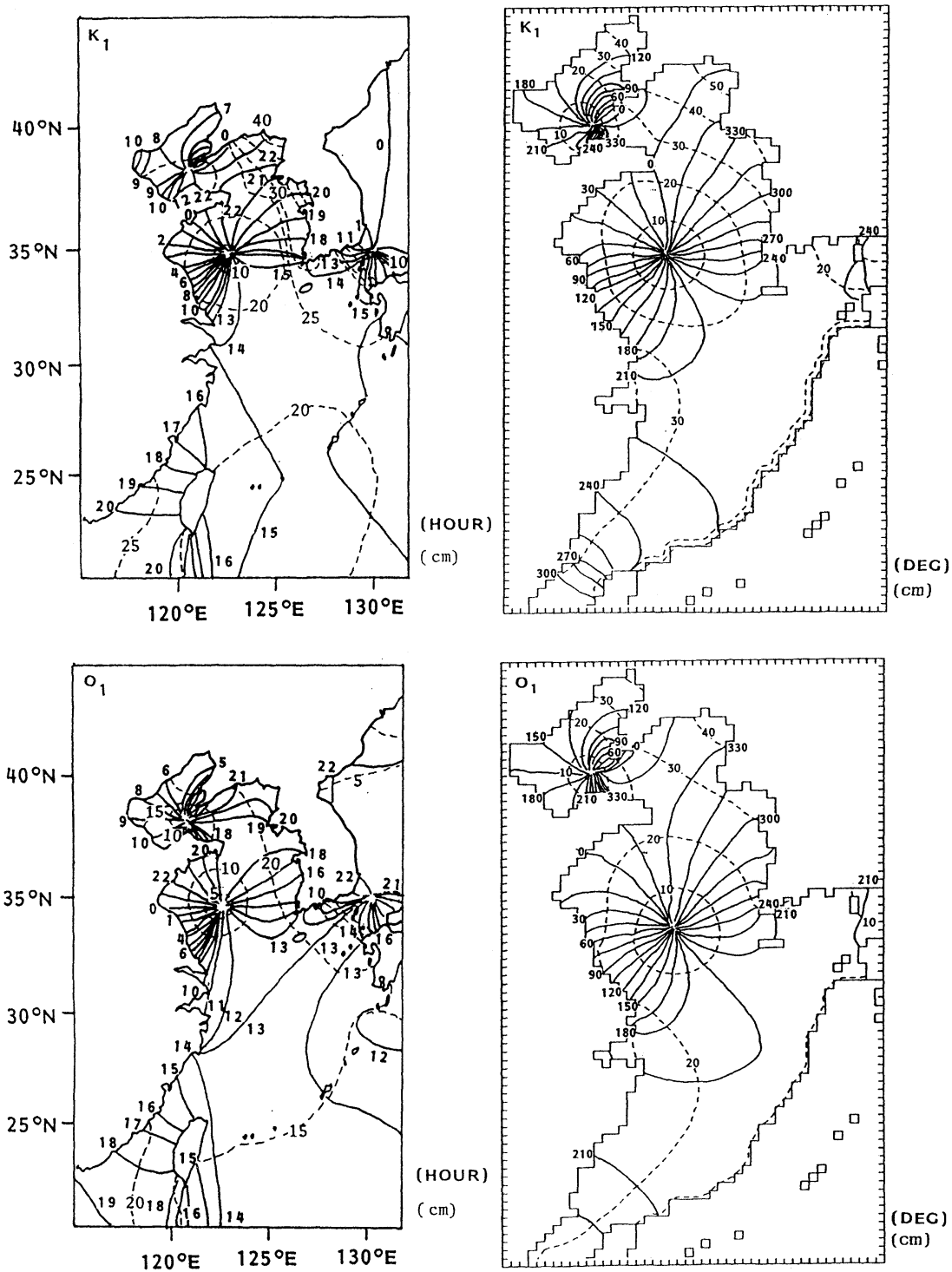


Fig. 4. Observed co-tidal (full line) and co-range (broken line) charts (left) and calculated ones right of K_1 and O_1 tides in the Yellow/East China Seas.

4. Results

4.1. Tides

The calculated co-tidal and co-range charts of four major component tides are shown in Fig. 4 with the observational results by NISHIDA (1980). As for N_2 tide, its co-tidal and co-range charts are very similar to those of M_2 and S_2 except the absolute values and they are not shown here. Calculated result of M_2 tide well coincides with the observed ones except an amphidromic point in Liautung Bay. The numerical experiment by AN (1977), which includes the tide-generating potential in the Yellow Sea and Bohai Sea, could not reproduce an amphidromic point of M_2 tide in Liautung Bay. AN (1977) showed that the tidal amplitude due to tide-generating potential was only about 3 % compared to that due to the incident tidal wave from the Pacific Ocean. Therefore, the disagreement of an amphidromic point of M_2 tide in Liautung Bay between the prototype and our numerical model is not due to the neglect of tide-generating potential. Also, such disagreement is not due to the employment of cartesian coordinate of our model because an amphidromic point of M_2 tide in Liautung Bay was not reproduced by CHOI (1980) with the spherical coordinate neglecting the tide-generating potential. The amphidromic point of S_2 tide in Liautung Bay is also not reproduced as shown in Fig. 4. The formation of amphidromic point is the problem of reflection of Kelvin wave at the back of the bay. LARSEN *et al.* (1985) inferred that such discrepancy of amphidromic point between the prototype and the numerical model might be due to poor grid resolution and the unnatural orientation of the grid system with respect to the coastal shape. Anyway, the reproduction of amphidromic point of semi-diurnal tides in Liautung Bay will be a future problem to be solved.

The amplitude of M_2 tide is over 160 cm at Seohan Bay, Kyonggi Bay (Inchon Bay is situated at the head of Kyonggi Bay) and Hangzhou Bay. The amplitude of S_2 tide exceeds 80 cm at the same places. AN (1977) showed that the resonance of semi-diurnal tide occurred in Kyonggi Bay, where the period of normal oscillation $T = 4L/(gH)^{1/2}$ (L : length of the bay = 100 km and H : the depth of the bay = 10 m)

was about 10 hours and it was very near that of semi-diurnal tides, and the tidal range was unstably amplified in the frictionless case. CHOI (1980) showed that such resonance was not occurred in the case of no Coriolis force because the propagation characteristic of M_2 tidal wave in the Yellow Sea was completely changed.

As for K_1 and O_1 tides, the calculated results well reproduce the observed one as shown in Fig. 4. The amplitude of K_1 and O_1 tides are over 40 cm and 30 cm, respectively, at the head of Liautung Bay and in Seohan and Kyonggi Bays. Amphidromic points of K_1 and O_1 tides are situated in the central part of the Yellow Sea while those of M_2 and S_2 tides near the Chinese Coast. Such facts suggest that the friction to diurnal tide is smaller than that to semi-diurnal tide in the Yellow Sea.

4.2. tidal currents

The current patterns of M_2 tidal current at the times of maximum flood and maximum ebb near the mouth of Changjiang are shown in Fig. 5 (a). The phase lag of M_2 tidal current between southern Chinese coast and Kyonggi Bay is about 180 degree, that is, the maximum flood current occurs in Kyonggi Bay when the maximum ebb current along the southern Chinese coast. The phase lag between Kyonggi Bay and Seohan Bay is also about 180 degree as shown later. S_2 tidal current has nearly the same pattern as M_2 tidal current except the maximum current speed of 40 to 50 cm s^{-1} (not shown). The current patterns of K_1 tidal component at the times of maximum flood and maximum ebb near the mouth of Changjiang are shown in Fig. 5 (b). The maximum current speed is about 20 cm s^{-1} and the strong current does not occur along the Korean coast. This may be due to the near-resonant response is only occurred in the period of M_2 or S_2 tidal components in Kyonggi Bay.

The comparisons of calculated tidal current ellipses and observed ones (CHOI, 1986) at some representative stations, shown in Fig. 3, are shown in Fig. 6 (a) and (b). The full circle in the left part shows the observational result, the dotted one in the left the calculated one by CHOI (1986) and the full circle in the right our result. The calculated M_2 and K_1 tidal current ellipses

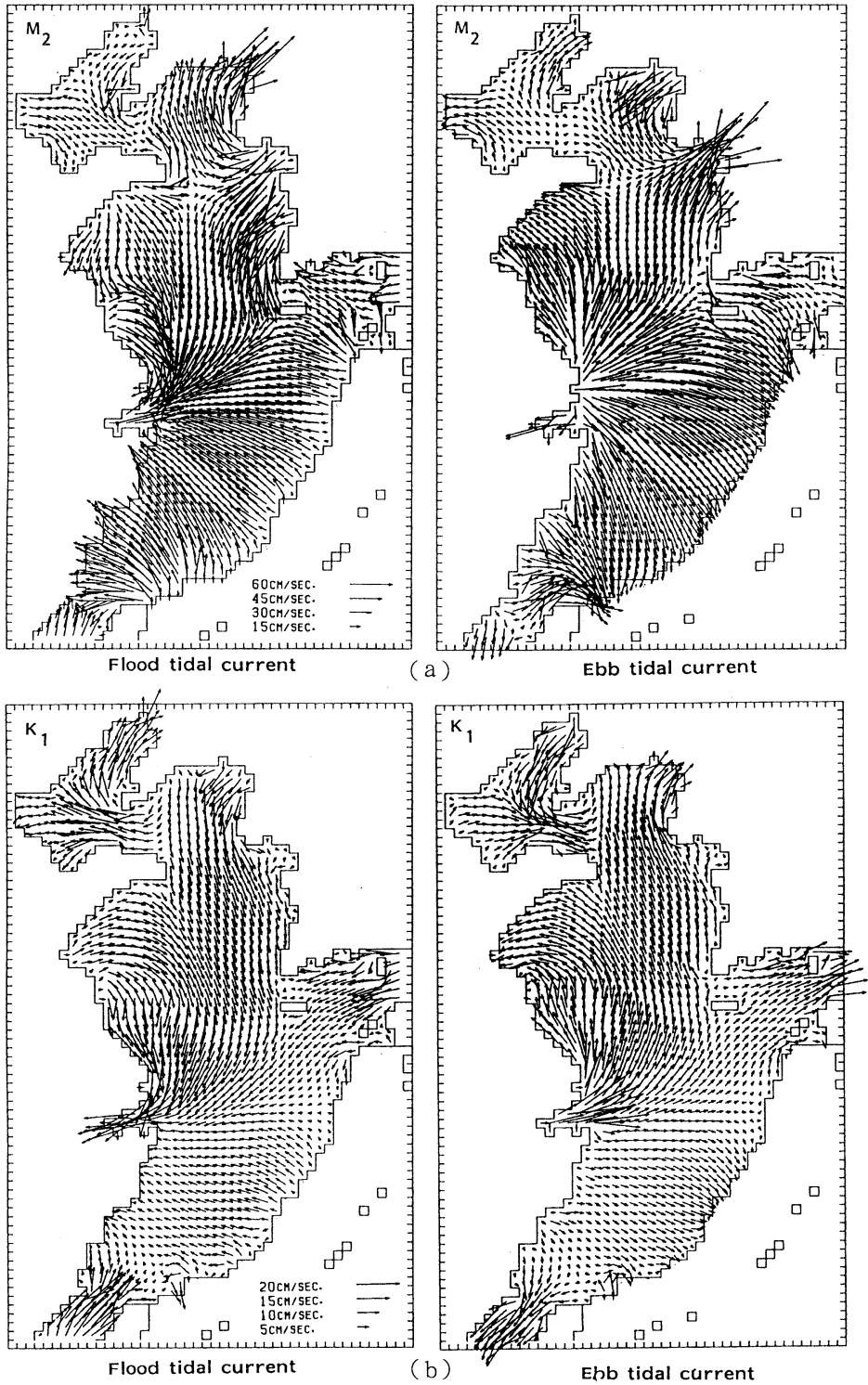


Fig. 5. Maximum flood (left) and ebb (right) tidal current at the river mouth of Changjiang in M_2 (a) and K_1 (b) components.

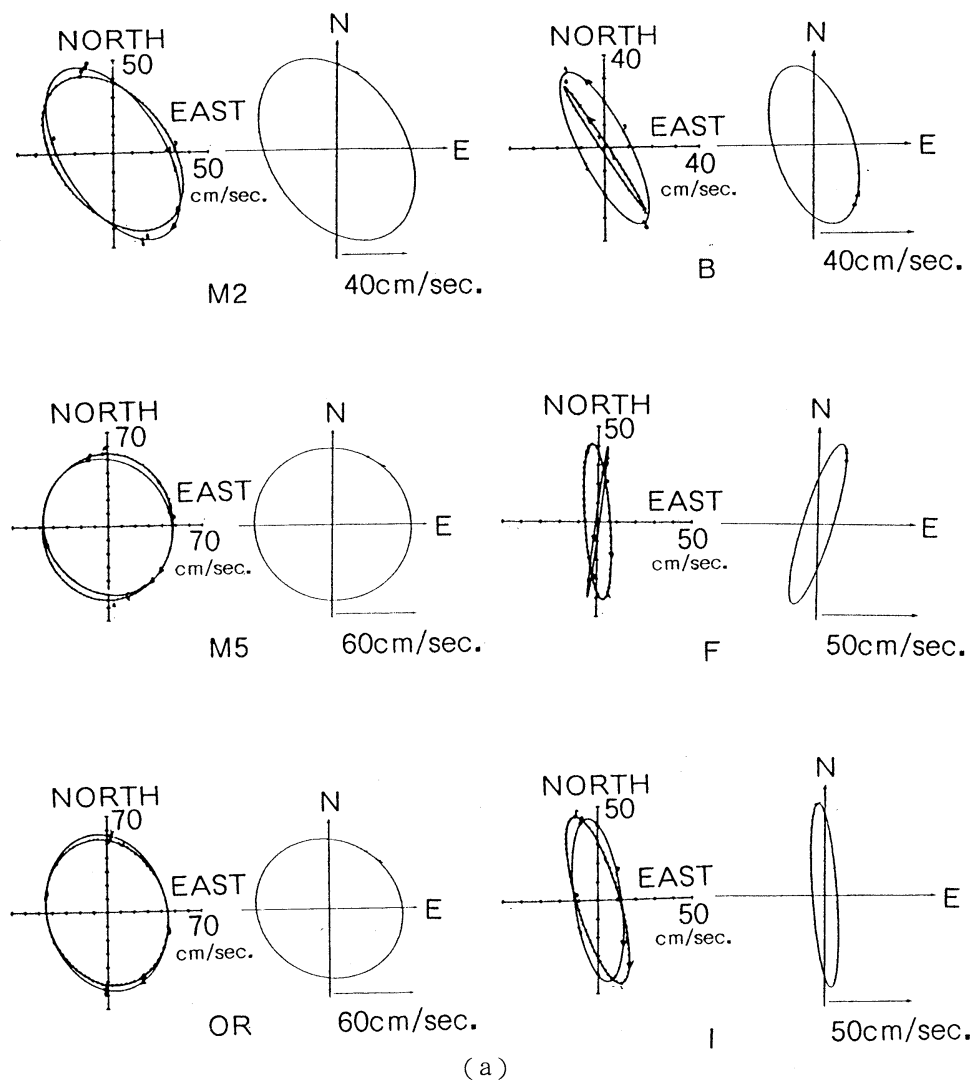
M_2 tidal ellipses

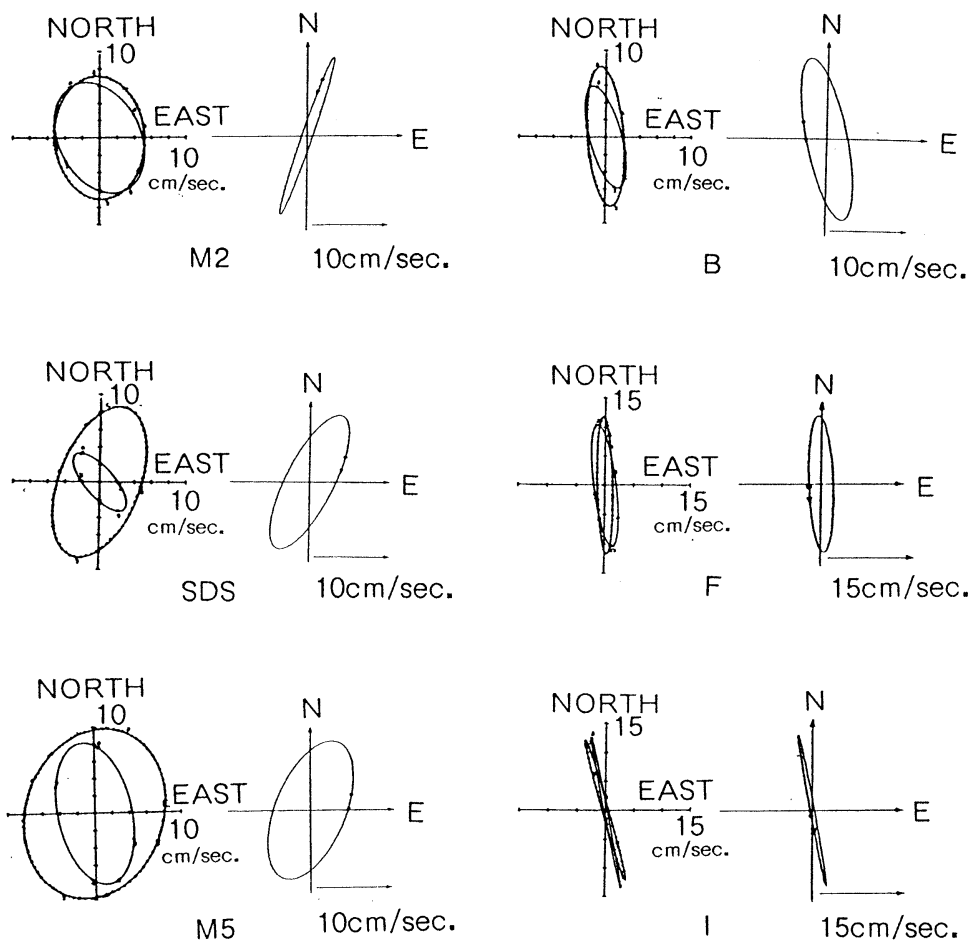
Fig. 6. Observed (full line in the left), calculated by CHOI (1986) (dotted line in the left) and calculated in the present model (full line in the right) M_2 (a) and K_1 (b) tidal current ellipses at representative stations shown in Fig. 3.

by our model well reproduce the observed ones and they are similar to those by CHOI (1986) as shown in Fig. 6.

The co-tidal and co-amplitude charts of four major tidal current components are shown in Fig. 7. The amplitudes of M_2 and S_2 tidal

currents are over 80 cm s^{-1} and 50 cm s^{-1} , respectively, in Seohan, Kyonggi and Hangzhou Bays and at the southwestern tip of Korea Peninsula. The amplitudes of K_1 and O_1 tidal currents are over 20 cm s^{-1} at the mouth of Bohai Sea and in Hangzhou Bay.

K₁ tidal ellipses



(b)

Fig. 6. Observed (full line in the left), calculated by CHOI (1986) (dotted line in the left) and calculated in the present model (full line in the right) M₂ (a) and K₁ (b) tidal current ellipses at representative stations shown in Fig. 3.

4.3. Tide-induced residual currents

The calculated tide-induced residual currents by M₂ and K₁ tides, which were obtained by averaging calculated tidal currents over one-tidal cycle, are shown in Fig. 8. The speed of tide-induced residual currents are very weak, that is, they are less than 2 cm s⁻¹ in the central part of Yellow/East China Seas except the particular

regions, e.g. at the mouth of Bohai Sea in the case of K₁ tide and at the south-western tip of Korea Peninsula in the case of M₂ tide. We cannot find the remarkable large-scale tide-induced residual circulations in the central part of Yellow/East China Seas from Fig. 8.

We carried out the same experiments with the cartesian co-ordinate of f-plane (that is, the

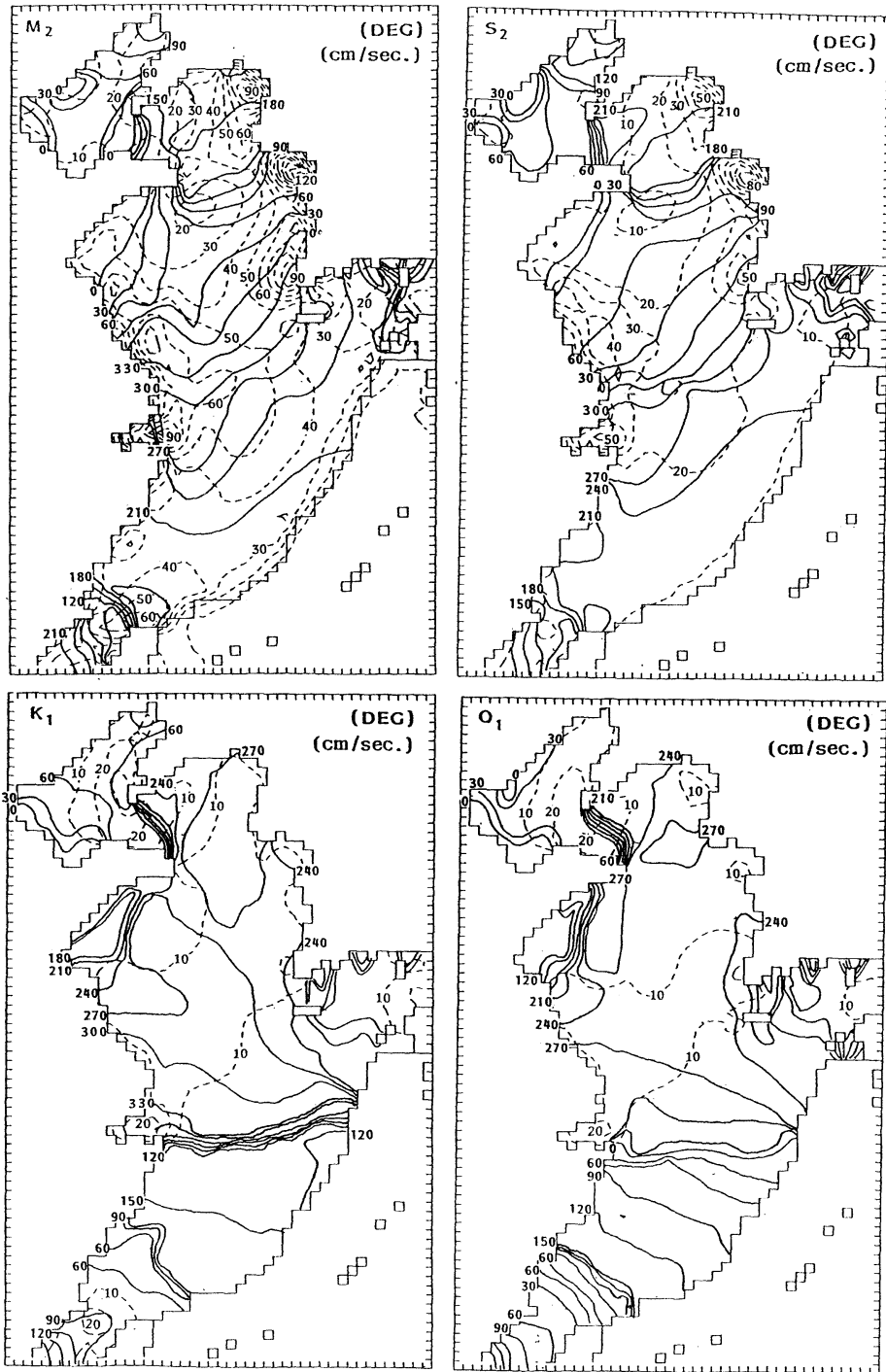


Fig. 7. Calculated co-tidal (full line) and co-amplitude (broken line) charts of M_2 , S_2 , K_1 and O_1 tidal currents.

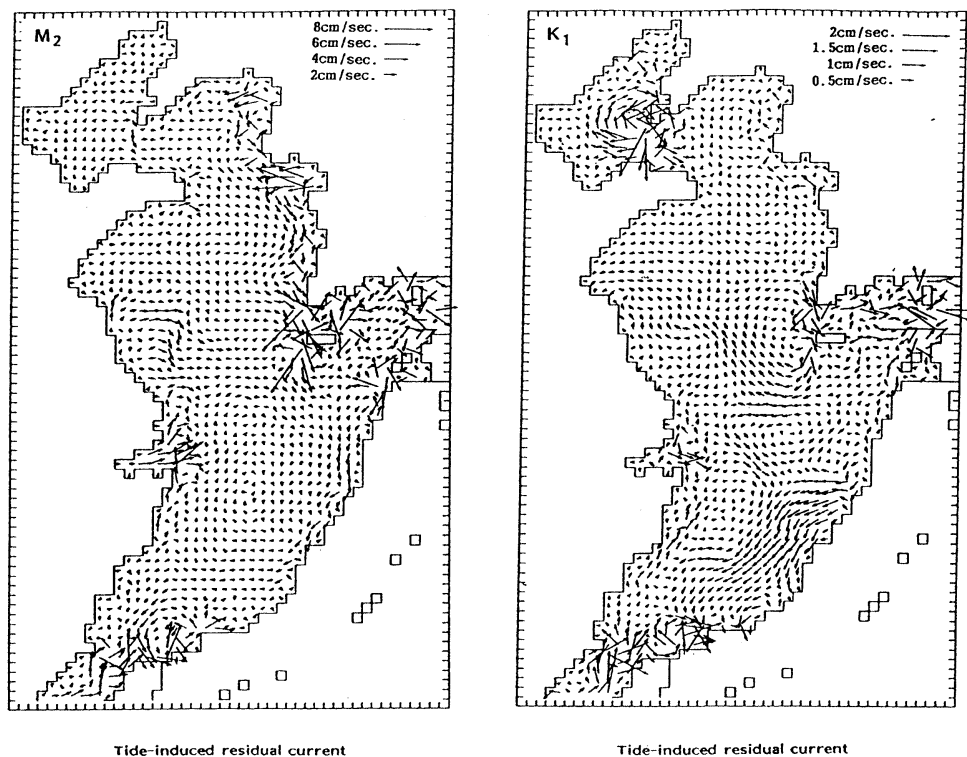


Fig. 8. Calculated tide-induced residual current of M_2 (left) and K_1 (right) tidal component.

Coriolis parameter is constant), but the results were nearly the same (not shown).

5. Conclusion

We developed two-dimensional numerical model under the cartesian co-ordinate of β -plane in the Yellow/East China Seas and compared its results with those of field observations and those of CHOI (1980 and 1986). The calculated tides and tidal currents of four major tidal components by our model well reproduce the observed ones and they are nearly the same as those of CHOI (1980 and 1986) which used the spherical co-ordinate of β -plane. We also carried out the numerical experiments with f -plane, but the calculated results are nearly the same as those with β -plane. Such results suggest that the curvature of the earth (spherical co-ordinate and β -effect) dose not affect the tidal phenomena in the Yellow/East China Seas.

Acknowledgments

The authors express their sincere thanks to Dr. H. TAKEOKA of Ehime University for his useful discussions, to Mr.S.TAKAHASHI for his help in numerical experiments and to Prof. B. H. CHOI for sending many valuable reprints. This study is a part of MASFLEX funded by the Agency of Science and Technology, Japan.

References

- AN, H.S. (1977): A numerical experiment of the M_2 tide in the Yellow Sea. *J. Oceanogr. Soc. Japan*, **33**, 103-110.
- CHOI, B.H. (1980): A tidal model of the Yellow Sea and the eastern China Sea. *KORDI Report 80-02*, 72p.
- CHOI, B.H. (1984): A three-dimensional model of the East China Sea. In "Ocean Hydrodynamics of the Japan and East China Seas" T. ICHIE (ed), Elsevier, Amsterdam, 209-224.
- CHOI, B.H. (1986): Predictions of sand transport directions of the offshore tidal sand banks in

- the Yellow Sea. 5th Congress Asian and Pacific Regional Division International Association for Hydraulic Research, 231-247.
- LARSEN, L.H., G.A. CANNON and B.H. CHOI (1985): East China Sea tidal currents. *Cont. Shelf Res.*, **4**, 77-103.
- NISHIDA, H. (1980): Improved tidal charts for the western part of the north Pacific Ocean. *Report of Hydrographic Researches*, **15**, 55-70.
- OGURA, S. (1933): The tides in the sea adjacent to Japan. *Bulletin of the Hydrographic Department, Imperial Japanese Navy*, **7**, 1-189.
- OGURA, S. (1941): Tides. Iwanami Co., Tokyo, 252 pp. (in Japanese).
- YANAGI, T. and Y. OKAMOTO (1985): A numerical simulation of oil spreading on the sea surface. *La mer*, **22**, 137-146.
- YANAGI, T. and S. TAKAHASHI (1993): Seasonal variation of circulations in the East China Sea and the Yellow Sea. *J. Oceanogr.*, **49**, 503-520.

黄海・東シナ海の潮汐・潮流

柳 哲雄・井上 康一

要旨 : 水平2次元 β 平面デカルト座標を用いた数値モデルで黄海・東シナ海の潮汐・潮流を計算した。Liutung 湾の半日周潮の無潮点が計算により再現されないことを除けば4大分潮の計算結果は観測結果をよく再現した。又この計算結果はf平面の結果やCHOI (1980) の水平2次元球面座標の結果とほとんど同一である。このことは地球の曲率は黄海・東シナ海の潮汐潮流現象にほとんど影響していないことを示唆している。